Disordered Magnetism at the Metal-Insulator Threshold in Nano-Graphite-Based Carbon Materials

Yoshiyuki Shibayama, Hirohiko Sato, and Toshiaki Enoki
Department of Chemistry, Tokyo Institute of Technology, 2-12-1 Ookayama, Meguro-ku, Tokyo 152–8551, Japan

Morinobu Endo
Department of Electrical Engineering, Shinshu University, 500 Wakasato, Nagano-shi, Nagano 380–8553, Japan
(Received 26 April 1999)

The magnetism of activated carbon fibers composed of a disorder network of nanographites was investigated, where each nanographite has about 1 edge-inherited localized spin. The susceptibility, for samples situated around the metal-insulator threshold, shows a cusp around 4–7 K in addition to the presence of a field-cooling effect. These behaviors are explained in terms of disordered magnetism caused by random strengths of inter-nano-graphite antiferromagnetic interactions mediated by π-conduction carriers.

PACS numbers: 71.24.+q, 75.30.Et, 75.50.Kj, 75.50.Lk

Nanosized particles, with sizes intermediate between molecules and bulk solids, are intriguing due to their novel electronic features depending on the sizes, shapes, surface conditions, and charging effects. Recently, nanosized graphite with open edges has been focused as the target of studies in relation to fullerenes and carbon nanotubes with close shaped π-electron systems. For the nanographite, Yoshizawa *et al.* [1] and Fujita *et al.* [2–4] predict the existence of an edge state of nonbonding π-orbital origin around the Fermi level. According to their works, the edge shapes govern the electronic state of the nanographite, with only zigzag edges giving rise to the edge state. Hence, the presence of the edge state is expected to give unique features to the electronic state of a nanographite, different from polycyclic aromatic hydrocarbons and bulk graphite which are present at the two extremes of these π-electron systems. Meanwhile, activated carbon fibers (ACFs) are known to be described by a three-dimensional disorder network of nanographites with a mean in-plane size of 30 Å [5–7]. Thus, they are interesting model materials expected to show the novel electronic state predicted by the theoretical studies. Previous works [8,9] profile their novel electron transport properties featured with Coulomb gap variable-range hopping [10] of π electrons between the nanographites. The heat treatment over 1300 °C generates percolative carrier conduction paths in the nanographite network, resulting in the metallic conduction. The heat treatment affects the magnetism of the ACFs as well, where the localized spins observed in as-prepared ACFs are diminished rapidly by heat treatment over 1300 °C [9]. In general, the origin of the spins in carbon materials has been assigned to the σ-dangling bonds of sp^3 C—C bond [11], although the details have not been clarified yet. Meanwhile, recent theoretical studies indicate that the edge states are localized on the zigzag edge-carbon atoms, and give paramagnetism [4]. Hence, these predictions give a new possibility for the origin of the spins in carbon materials. In the present work, detailed behavior of magnetism in the ACFs is investigated with special attention given to the insulator-metal (*I-M*) threshold, in order to clarify the electronic and magnetic features of the networked nanographites and the nanographite itself.

Pitch-based ACFs having specific surface areas of 1500 $m^2\,g^{-1}$ (Osaka Gas Company, A15) were used as samples. The susceptibility measurements were performed with a SQUID magnetometer in the temperature range of 2–380 K under the magnetic field up to 5.5 T after the following sample setup. A bundle of 15 mg sample, wadded in the center of a quartz tube with a closed end, was vacuum sealed after the vacuum heat treatment at the heat treatment temperature (HTT) of 800 °C and at 1×10^{-6} Torr for 1 h for removing adsorbed gases. The susceptibility was measured with the sample (named HTT800) kept in a vacuum tube in order to avoid gas adsorption. After the measurements, the HTT800 sample was re-heat-treated for 15 min at 900 °C, and then the measurements were performed again. Similar procedures were taken successively up to 1500 °C. Finally, heat treatment at 1500 °C for 1 h [HTT1500(1h)] was carried out as the most intensive heat treatment in the series of the experiments.

Figure 1(a) gives the temperature dependence of the susceptibility χ for HTT800-1500(1h) under $H = 1$ T. A possibility of the contamination of magnetic impurities can be excluded because of the complete fidelity in the behavior of χ to the *I-M* transition around HTT 1100–1200 °C [9]. For the HTT $\leq$ 1100 °C samples (L-HTT ACFs), χ obeys the Curie-Weiss law in the whole temperature range investigated, while χ for the HTT $\geq$ 1200 °C samples (H-HTT ACFs) deviates from the Curie-Weiss law below about 20 K and gives a cusp around 4–7 K. Moreover, further heat treatment in the metallic region makes the cusp depressed, in addition to a negative shift in χ. In the temperature range where χ obeys the Curie-Weiss law, a least square fit was performed based upon the

 0031-9007/00/84(8)/1744(4)$15.00

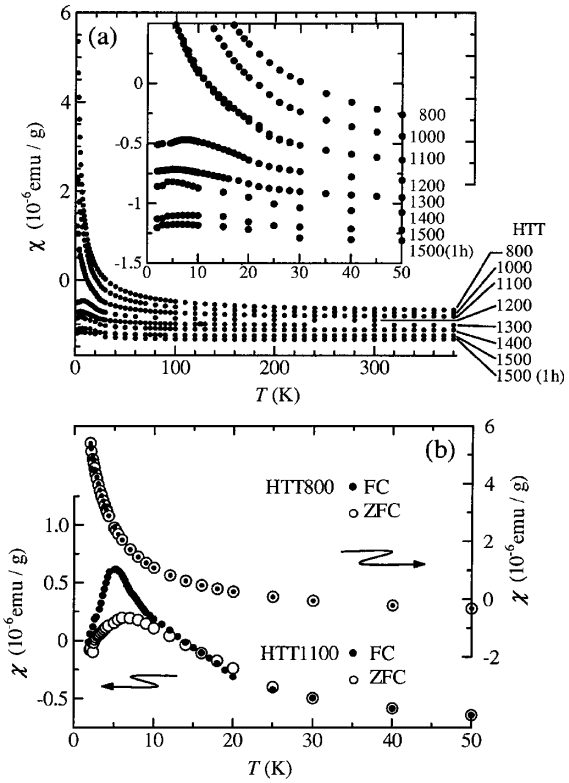

FIG. 1. (a) Temperature dependence of the susceptibility χ under $H = 1$ T for the ACFs vacuum heat treated up to 1500 °C. Detailed behavior at low temperatures is shown in the inset. (b) Field cooling effects on χ for HTT800 and HTT1100 under $H = 1$ T. The measurements were performed in heating runs after the cooling processes down to 2 K with $H = 0$ (○) and 1 T (•).

assumption that the observed χ is the sum of the Curie-Weiss term $C/(T - \Theta)$ and the temperature-independent term χ_0, where C and Θ are the Curie constant and the Weiss temperature, respectively. Here, $S = 1/2$ and $g = 2$ are taken since the spins are associated with carbon materials. The fitting results, along with the spin density per 1 g of ACFs N_s, the number of spins per nanographite n, Θ, and χ_0, are shown in Fig. 2, where n is estimated using the nanographite in-plane size [9]. The heat treatment makes N_s decrease considerably from 4.2×10^{19} g^{-1} (HTT800) to 0.39×10^{19} g^{-1} [HTT1500(1h)]. The constant term χ_0 is negative and its absolute value is enhanced upon the heat treatment from -0.73×10^{-6} emu g^{-1} (HTT800) to -1.36×10^{-6} emu g^{-1} [HTT1500(1h)]. In contrast, Θ has similar negative values in the range of -2 to -3 K irrespective of HTT, proving the presence of antiferromagnetic interactions. Figure 3(a) shows the magnetization curves (M-H curves) at 2 K. The M-H curves for the L-HTT ACFs show a Brillouin-curve type saturating trend in the high magnetic field, indicating the localized spin feature. In contrast, the magnetizations for the H-HTT ACFs are almost proportional to the field with the presence of a slight concavity [Fig. 3(b)]. This

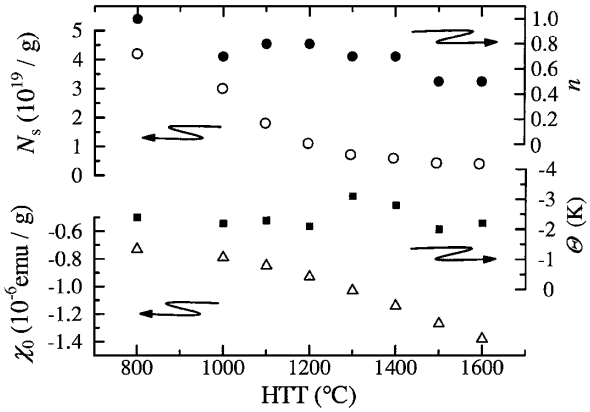

FIG. 2. The spin density N_s (○) , the number of spins per nano-graphite n (•), the Weiss temperature Θ (■), and the temperature-independent susceptibility term χ_0 (△) for all the samples shown in Fig. 1(a). The data for HTT1500(1h) are positioned at HTT = 1600 °C for clarity.

behavior cannot be explained with isolated localized spins, but is reminiscent of the M-H curve in an antiferromagnetic ordered state. Figure 1(b) shows the field-cooling effect on χ for HTT800 and HTT1100, prepared independently of those used in the experiments in Figs. 1(a) and 3. The measurements were carried out under $H = 1$ T in heating runs after cooling processes from room temperature to 2 K with fields of $H = 0$ and 1 T. In HTT800, χ obeys the Curie-Weiss law without a field-cooling effect, while HTT1100 having a cusp shows a remarkable difference below 15 K between the zero field and the field coolings; that is, the field cooling enhances the cusp.

We first discuss the origin of the spins in the ACFs. The spin density N_s is diminished greatly from 4.2×10^{19} to 0.39×10^{19} g^{-1} by the heat treatment up to 1500 °C. In contrast, the number of spins per nanographite n shows a more moderate decrease from 1 to 0.5 because of the

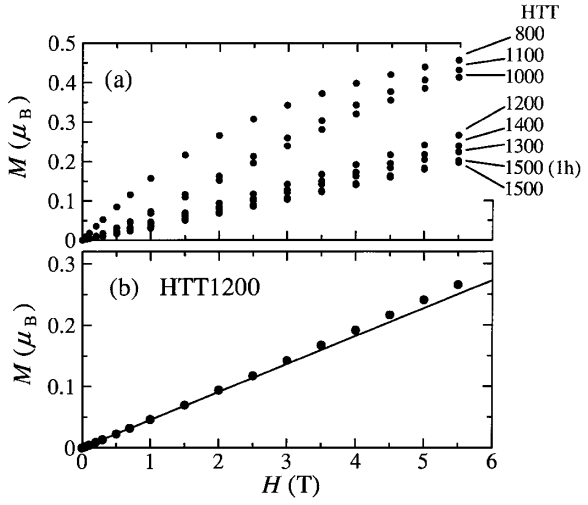

FIG. 3. (a) Magnetization curves at 2 K for all the samples shown in Fig. 1(a). The contribution of χ_0 has been subtracted. (b) Detailed magnetization curves at 2 K for HTT1200. The solid line shows a linear line for the least square fit below 1 T.

growth of the nanographite in-plane size L_a from 25 to 52 Å by the heat treatment. Hence, each nanographite has about 1 spin irrespective of L_a, suggesting the important role of nanographite edges in the origin of the spins. In general, the localized spins of disorder carbons, composed of sp^2 and sp^3 C—C bond network, have been considered to originate from σ-dangling bonds [11]. The origin of the spins, however, remains unverified since the σ-dangling bonds of carbon atom are too chemically active to be stabilized in the atmospheric condition. In particular, the nanographite in the ACFs is composed of well-characterized condensed aromatic rings with few sp^3 bonds forming nanographite bridges [5–7]. Moreover, in relation to the appearance of novel magnetism in nanographites, recent theoretical studies predict the presence of nonbonding π-electron edge states, which are localized on peripheral carbon atoms composing zigzag edges, even if these carbon atoms are terminated by foreign atoms such as hydrogen [2–4]. These predictions have been reinforced by recent experiments evidencing the novel edge-state-based magnetism [12]. Hence, judging from the theoretical and experimental studies, the spins observed in the present work are considered to originate from the nonbonding edge states of the π electron.

Next, we discuss the exchange interaction in the nanographite network. According to the behaviors of the magnetism depending on HTT, the samples can be classified into two groups: L-HTT and H-HTT samples, bordered at the *I-M* percolation threshold HTT1100–HTT1200. For the L-HTT ACFs which are below the threshold, χ obeys the Curie-Weiss law with negative Weiss temperatures and the *M-H* curves show a Brillouin-curve-type saturating trend. Thus, the magnetization M is analyzed by the Brillouin function with the antiferromagnetic internal field H_{int}; $M = N\mu_{\text{B}} \tanh[\mu_{\text{B}}(H + H_{\text{int}})/(k_{\text{B}}T)]$, where μ_{B} and k_{B} are the Bohr magneton and the Boltzmann constant, respectively. H_{int} is associated with the observed Weiss temperatures; $H_{\text{int}} = \alpha M$, $\alpha \equiv \Theta/C$. For HTT800 the calculated curve (line *A*) is shown in Fig. 4(a) with the experimental results. Line *A* gives larger magnetizations than the observed ones in the whole field range in addition to a less saturating trend in the high field. Namely, the Brillouin curve with a unique internal field does not fully represent the experimental results. This discrepancy can be interpreted by the disorder structure of the ACFs, where the strengths of the exchange interactions are considered to depend on the locations of spins, varying randomly. In order to make the analysis more realistic, we introduce the distribution function $P(\alpha)$ for representing randomness of the exchange interactions. $P(\alpha)$ is assumed to be a normal distribution, where ferromagnetic interaction ($\alpha > 0$) is cut off because of the absence of ferromagnetic interactions in the present case. The least square fit is performed with two adjustable parameters; the center and the dispersion of $P(\alpha)$. Line *B* in Fig. 4(a)

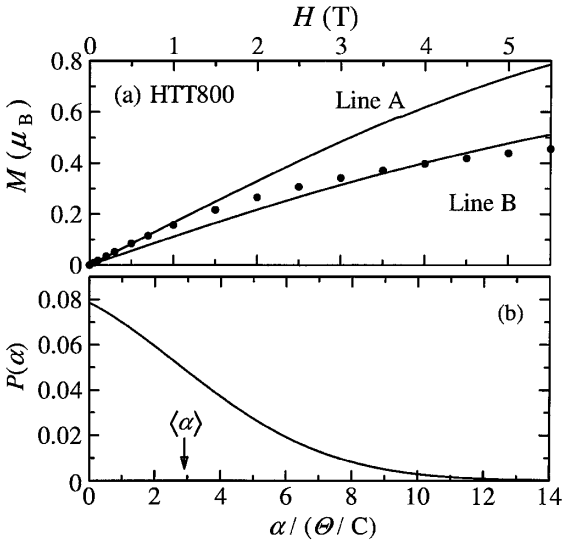

FIG. 4. (a) Magnetization curve at 2 K of HTT800 (•) and the two fitting curves (solid lines). Line *A* is the Brillouin curve fitting with a unique molecular field constant $\alpha = \Theta/C$, while line *B* gives the Brillouin curve where the strengths of α are assumed to be randomly distributed as shown in (b). (b) The distribution function $P(\alpha)$ of α used in the fitting of line *B*. The arrow with $\langle\alpha\rangle$ indicates the mean value (see text).

gives the fitting results. Introducing $P(\alpha)$ considerably improves the fitting results in contrast with line *A*, and the saturating trend in M is well reproduced. However, there still remains a discrepancy between the calculation and observation that might come from a deviation of $P(\alpha)$ from the normal distribution feature. The fitting result gives an estimate of $|\sqrt{\langle\Delta\alpha^2\rangle}/\langle\alpha\rangle| \sim 0.8$, suggesting the presence of a large randomness in the strengths of the exchange interactions. The exchange interactions with random strengths provide a favorable trend to a disordered magnetic state like a spin glass state [13] for the ACFs spin system. In this connection, the inspection of χ is diagnostically important. For HTT800, χ shows typical Curie-Weiss behavior with no field-cooling effect, being ordinary localized electron magnetism. This is reasonably understood by the fact that the ACFs below the percolation threshold such as HTT800 have no infinite exchange interaction network. Interestingly, above the threshold, the magnetic features change drastically; that is, the deviation from the Curie-Weiss behavior, the presence of a cusp and its field-cooling effect in addition to a slight concavity in the *M-H* curve similar to that for an antiferromagnetic ordered state. These features in the magnetism demonstrate the formation of a disordered magnetic state similar to a spin glass state around the percolation threshold where an infinite network of random antiferromagnetic interactions develops.

The existence of the discrepancy in the susceptibility between the zero-field cooling and the field cooling is a characteristic feature of a spin glass state. The observed

field-cooling effect, however, deviates from that of the ordinary spin glass behavior which does not show any decreasing trend in χ on the low temperature side of the cusp in the field-cooling condition [13]. In the present case, it is considered that a competition between antiferromagnetic ordering and disordered magnetism interferes with the formation of a prototypical spin glass transition. In addition, taking into account that the exchange interaction between the spins is mediated by the percolating conduction π electron, which will be discussed in the next paragraph, the dimensionality of the present spin system becomes considerably lowered in the vicinity of the *I-M* percolation threshold [14,15], at which the novel magnetism appears. Therefore, the low dimensionality of the exchange interaction path network might remove a true spin glass feature from the present spin system [16,17].

Finally, we discuss the origin of the exchange interaction in relation to the interplay between the edge states and the conduction π electrons. Since each nanographite has about 1 spin, the mean distance between the spins is in the same range as $L_a \sim 30$ Å. Hence, there is no direct exchange interaction between the spins. The metallic conduction above the percolation threshold is caused by the conduction of π electrons through percolative conduction paths. Thus, the exchange interaction between localized nonbonding π electrons at the edge states is considered to be mediated by conduction of π electrons, similar to the *s-d* interaction in transition metal magnets. The considerably enhanced electronic specific heat having a large magnetic field dependence in disordered graphite [18] supports the evidence of the conduction-π-electron-mediated interaction. The disorder network of the nanographites forms a random exchange interaction network, resulting in the appearance of disordered magnetism like a spin glass behavior driven by the antiferromagnetic interactions in the vicinity of the *I-M* threshold. The decreasing trend in the spin concentration above the *I-M* threshold suggests the fusion of nanographite domains and/or the presence of charge transfer interaction between the edge states and the π bands, which are favorable for the development of the conduction-electron-mediated interaction network. Heat treatment over 1500 °C promotes graphitization of ACFs, resulting in the disappearance of the edge states. Eventually, the stabilization of metallic state at the expense of the edge states makes the disordered magnetism wiped out well above the *I-M* threshold, and the magnetism becomes subjected to the Pauli paramagnetism and the orbital diamagnetism caused by itinerant π electrons [9].

In summary, the magnetism of the ACFs composed of a nanographite disorder network is explained in terms of antiferromagnetically interacting spins, which originate from the nonbonding π electrons of nanographite edge origin. In the vicinity of the *I-M* percolation threshold, a novel edge-state-based disordered magnetism similar to a spin glass state appears. The considerably long range exchange interaction varying randomly is considered to be mediated by conduction π electrons similar to *s-d* interaction in transition metal magnets. The non-bonding-π-electron-based disordered magnetism in the nanographite system provides a new class of magnetism that has never been reported.

The authors express their gratitude to Dr. N. Shindo at Osaka Gas Company for providing ACF samples, and to Professor M. Matsuura, Professor H. Nishimori, and Professor M. Suzuki for valuable discussion. Y. S. was supported by JSPS. The present work was supported by the Grant-in-Aid for "Research for the Future Program," Nano-carbons, from JSPS.

[1] K. Yoshizawa, K. Okahara, T. Sato, K. Tanaka, and T. Yamabe, Carbon **32**, 1517 (1994).
[2] M. Fujita, K. Wakabayashi, K. Nakada, and K. Kusakabe, J. Phys. Soc. Jpn. **65**, 1920 (1996).
[3] M. Fujita, M. Igami, and K. Nakada, J. Phys. Soc. Jpn. **66**, 1864 (1997).
[4] K. Wakabayashi, M. Fujita, H. Ajiki, and M. Sigrist, Phys. Rev. B **59**, 8271 (1999).
[5] M. S. Dresselhaus, A. W. P. Fung, A. M. Rao, S. L. di Vittorio, K. Kuriyama, G. Dresselhaus, and M. Endo, Carbon **30**, 1065 (1992).
[6] K. Kuriyama and M. S. Dresselhaus, J. Mater. Res. **6**, 1040 (1991).
[7] A. M. Rao, A. W. P. Fung, M. S. Dresselhaus, G. Dresselhaus, and M. Endo, J. Mater. Res. **7**, 1788 (1992).
[8] A. W. P. Fung, Z. H. Wang, M. S. Dresselhaus, G. Dresselhaus, R. W. Pekala, and M. Endo, Phys. Rev. B **49**, 17 325 (1994).
[9] Y. Shibayama, H. Sato, T. Enoki, X. X. Bi, M. S. Dresselhaus, and M. Endo, J. Phys. Soc. Jpn. (to be published).
[10] A. L. Efros and B. I. Shklovskii, J. Phys. C **8**, L49 (1975).
[11] I. C. Lewis and L. S. Singer, *Chemistry and Physics of Carbon*, edited by P. L. Walker, Jr. and P. A. Thrower (Marcel Dekker, Inc., New York, 1981), Vol. 17, p. 1.
[12] O. E. Andersson, B. L. V. Prasad, H. Sato, T. Enoki, Y. Hishiyama, Y. Kaburagi, M. Yoshikawa, and S. Bandow, Phys. Rev. B **58**, 16 387 (1998).
[13] M. Mezard, G. Raris, and M. A. Virasoro, *Spin Glass Theory and Beyond* (World Scientific, New Jersey, 1987).
[14] R. A. Cowley, R. J. Birgeneau, and G. Shirane, *Ordering in Strongly Fluctuating Condensed Matter Systems*, edited by T. Riste (Plenum Press, New York, 1979).
[15] R. J. Birgeneau, R. A. Cowley, G. Shirane, J. A. Tarvin, and H. J. Guggenhein, Phys. Rev. B **21**, 317 (1980).
[16] R. R. P. Singh and S. Chakravarty, Phys. Rev. Lett. **57**, 245 (1986).
[17] R. R. P. Singh and S. Chakravarty, Phys. Rev. B **36**, 546 (1987).
[18] S. Mrozowski, J. Low Temp. Phys. **35**, 231 (1979).